DIRECT QUADRATURE METHOD OF MOMENTS FOR ISOTHERMAL BUBBLY FLOWS

Sherman C.P. CHEUNG[1], Guan H. YEOH[2] and <u>Jiyuan TU</u>[1][*]

[1] School of Aerospace, Mechanical and Manufacturing Engineering, RMIT University, VIC 3083, Australia
[2] Australian Nuclear Science and Technology Organization (ANSTO), NSW 2234, Australia
*Corresponding author, E-mail address: Jiyuan.TU@rmit.edu.au

ABSTRACT

Currently, the two-fluid model is one of the most practical and accurate macroscopic formulations for handling bubbly flow systems. Nevertheless, in order to rigorously account for bubble-bubble interactions (e.g. coalescence and breakage), the population balance equation (PBE) must be solved along with the continuity and momentum balance equations. Recently, the MUltiple SIze Group (MUSIG) model appears to be one of the most common and direct methods to solve the PBE with a finite series of discrete classes. Nonetheless, a large number of classes must be used posing severe limitations on the computational resources for complex bubbly flows. An attractive alternative is represented by the direct quadrature method of moments (DQMOM) (Marchisio and Fox, 2005) where the particle size distribution (PSD) is tracked through its moments by integrating out the internal coordinate. The main advantage of DQMOM is that the number of scalars to be solved is very small (i.e. usually 4-6). The objectives of this present study are: (1) to implement the DQMOM model to accommodate coalescence and breakage of bubbles, and (2) to validate the model against measurements of bubbly flows by Hibiki et al. (2001) for a range of flow conditions. Preliminary computed results compared very well against the experimental data.

NOMENCLATURE

a_{if}	interfacial area concentration
a	coalescence rate
b	breakage rate
B^c, B^b	birth rate due to coalescence and break-up
D^c, D^b	death rate due to coalescence and break-up
f	bubble size distribution function
F_i	total interfacial force
g	gravitational acceleration
j	superficial velocity
M	mass scale of gas phase (bubble)
N	number density of gas phase (bubble)
P	pressure
p	number of fragments/daughter bubbles
t	physical time
u	velocity
We	Weber number

Greek symbol

α	void fraction
δ	Dirac's delta function
ε	turbulence kinetic energy dissipation
μ^e	effective viscosity
ξ	internal space vector of the PBE
ρ	density
σ	surface tension
ψ	weighted abscissas

Subscripts

g	gas
i	Index of abscissas or gas/liquid phase
l	Liquid
min	Minimum operator
max	Maximum operator

INTRODUCTION

Two-phase flows are prevalent in many technological systems. In chemical industries, bubble column reactors are extensively used for handling processes that require large interfacial area and efficient mixing processes. Engineering systems such as heat exchangers widely employ two-phase flow mixture of gas and liquid for efficient removal of heat generation. In the nuclear area, the capability to predict void fraction profile and other two-phase flow parameters in subcooled boiling flows is of considerable importance to ensure the safe operation of the reactor.

In the present state-of-the-art, two-fluid model can be considered as one of the most practical and accurate macroscopic formulations to model the thermal-hydrodynamics of two-phase flow systems. Within the field equations, which are expressed by the conservation of mass, momentum and energy for each phase, interfacial transfer terms appear in each of the equations. These terms require essential closure relations and should be modelled accurately. Interfacial transfer terms in the two-fluid model are strongly related to the local transfer mechanisms such as the degree of turbulence near the interfaces and the interfacial area concentration. Theoretically speaking, the interfacial area concentration (a_{if}) is a geometrical parameter of the local interfacial structure which describes the available area for the interfacial mass, momentum and energy transport. All the above interfacial transport mechanisms between phases are proportional the local interfacial area concentration. However, the closure relations for the interfacial transfer terms remain far from resolution and they still represent the weakest link in the two-fluid model.

Since the interfacial area concentration represents the key parameter that links the interaction of the phases, much attention have been concentrated towards better understanding the coalescence and breakage effects due to interactions among bubbles and between bubbles and turbulent eddies for gas-liquid bubbly flows. The primary objective is to better describe the temporal and spatial evolution of the two-phase geometrical structure.

Population balance approaches (Cheung et al., 2008, Wang et al., 2005, Chen et al., 2004) and volumetric interfacial area transport equation (Hibiki and Ishii, 2000, Yao and Morel, 2004, Sun et al., 2004, Wu et al., 1998) have been proposed to predict the interfacial area concentration.

Benefitting from the early introduction to commercial package (Lo, 1996), the population balance approach based on the MUSIG model has been frequently employed to predict the non-uniform bubble size distribution in a gas-liquid mixture by solving a range of bubble classes. Although encouraging results have been reported (Chen et al., 2004, Cheung et al., 2007b), in case of wide range of bubble sizes in a complex two-phase flow system were being considered, a substantial number of equations might be required to adequately track the range of bubble sizes. For flows where large bubbles could exist, especially in large diameter pipe, computational resource for solving such large number of transport equations could be extremely excessive. This model drawback is fundamentally caused by the fact that it adopts class method to discretize the bubble size distribution where the pivot size or abscissa of each class is fixed. In practical calculations where the number of bubble classes is limited, bubble size distribution cannot be adequately represented.

In this paper, an alternative approach to predict gas-liquid bubbly flows is presented by the consideration of Method of Moments (MOM). Here, the bubble size distribution is tracked through its moments by integrating out the internal coordinates. The main advantage of MOM is its numerical economy that condenses the problem substantially by only tracking the evolution of a small number of moments (i.e. usually 4-6). As aforementioned, this becomes rather critical in modeling complex flow problems when the bubble dynamics is strongly coupled with already time-consuming calculations of turbulence multiphase flows. However, due to the difficulties related with expressing transport equations in terms of the moments themselves, the Direct Quadrature Method of Moments (DQMOM) is applied instead which essentially involves the direct solution of the transport equations for weights and abscissas of the quadrature approximation. As will become clearer later, each node of the quadrature approximation can be treated as a distinct gas phase. DQMOM, similar to MUSIG, thus offers a powerful approach for describing polydisperse bubbly flows undergoing coalescence and breakage processes in the context of Computational Fluid Dynamics simulations.

MODEL DESCRIPTION

Two-fluid model for gas-liquid flow

The three-dimensional two-fluid model solves the ensemble-averaged of mass and momentum transport equations governing each phase. These equations can be written as:

$$\frac{\partial(\rho_i\alpha_i)}{\partial t} + \nabla\cdot(\rho_i\alpha_i\vec{u}_i) = 0 \qquad (1)$$

$$\frac{\partial(\rho_i\alpha_i\vec{u}_i)}{\partial t} + \nabla\cdot(\rho_i\alpha_i\vec{u}_i\vec{u}_i) = -\alpha_i\nabla P + \alpha_i\rho_i\vec{g}$$
$$+ \nabla\cdot[\alpha_i\mu_i^e(\nabla\vec{u}_i + (\nabla\vec{u}_i)^T)] + F_i \qquad (2)$$

where $\vec{g}$ is the gravity acceleration vector and P is the pressure. From the above equation, it is noted that closure

law is required to determine the momentum transfer of the total interfacial force. This force strongly governs the distribution of the liquid and gas phases within the flow volume. On the L.H.S of equation (2), F_i represents the total interfacial force which is composed of the drag force, lift force, wall lubrication force and the turbulent dispersion force respectively. Numerical details on handling these interfacial forces can be found in Cheung et al. (2007a) and references therein. For handling the turbulence effects, the Shear Stress Transport (SST) model is adopted for the liquid phase (Menter, 1994), while the Sato's bubble-induced turbulent viscosity model (Sato et al., 1981) was employed for the gas phase.

Direct quadrature method of moments

For the PBE, an integrodifferential form describing the local Bubble Size Distribution (BSD) can be written as:

$$\frac{\partial f(\xi,t)}{\partial t} + \nabla\cdot(u(\xi,t)f(\xi,t)) = S(\xi,t) \qquad (3)$$

where $f(\xi,t)$ is the function of bubble size distribution dependent on the internal space vector ξ, whose components could be characteristics dimensions, surface area, volume and so on. t is the external variables representing the physical time in external coordinate respectively. $u(\xi,t)$ is velocity vector in external space.

The R.H.S of equation (3) is the net source or sink term of the PBE which denotes the birth and death rates of bubbles due to coalescence and breakage processes defined by:

$$S(\xi,t) = \frac{1}{2}\int_0^\xi a(\xi-\xi',\xi')f(\xi-\xi',t)f(\xi',t)d\xi'$$
$$- f(\xi,t)\int_0^\infty a(\xi-\xi',\xi')f(\xi',t)d\xi'$$
$$+ \int_\xi^\infty \gamma(\xi')b(\xi')p(\xi/\xi')f(\xi',t)ds$$
$$- b(\xi)f(\xi,t) \qquad (4)$$

Here, the first and second terms denote birth and death rate of bubble of space vector ξ due to coalescence processes; the third and fourth terms account for the birth and death rate caused by the breakage processes respectively. $a(\xi,\xi')$ is the coalescence rate between bubbles of size ξ and ξ'. Conversely, $b(\xi)$ is the breakage rate of bubbles of size ξ. $\gamma(\xi')$ is the number of fragments/daughter bubbles generated from the breakage of a bubble of size ξ' and $p(\xi/\xi')$ represents the probability density function for a bubble of size ξ to be generated by breakage of a bubble of size ξ'.

Like all method of moment approaches, the basic idea of DQMOM founded upon a transforming the problem into lower-order moments of the size distribution where the integral of the BSD function is approximated by a finite set of Dirac's delta functions (McGraw, 1997). Taking the bubble mass, M, as the internal coordinate, the BSD can then be expressed as:

$$f(M,t) \approx \sum_{k=1}^n N_k(t)\delta(M - M_k(t)) \qquad (5)$$

where N_k represents the number density or weight of the ith class and consists of all bubbles per unit volume with a pivot size or abscissa M_k. Obviously, the quadrature method is brought down to solving $2N$ unknowns, N_k and M_k. A number of approaches in the specific evaluation of the quadrature abscissas and weights have been proposed. With the aim to solve multi-dimensional problems, Marchisio and Fox (2005) extended the method by developing the DQMOM where the quadrature abscissas and weights are formulated as transport equations. The main idea of the method is to keep track of the primitive variables appearing in the quadrature approximation, instead of moments of the BSD. As a result, the evaluation of the abscissas and weights are obtained using matrix operations. More details of the method can be found in above reference.

In the present study, in order to be consistent with the variables used in the two-fluid model, the weights and abscissas can be related to the size fraction of the dispersed phase (f_k) and a variable defined as $\psi_k = f_k / M_k$. As a preliminary study, bubbles are assumed to travel with the gas velocity, the size fraction of f_k is related to the weights and abscissas by:

$$\rho_g \alpha_g f_k = N_i M_i = \zeta_k \qquad (6)$$

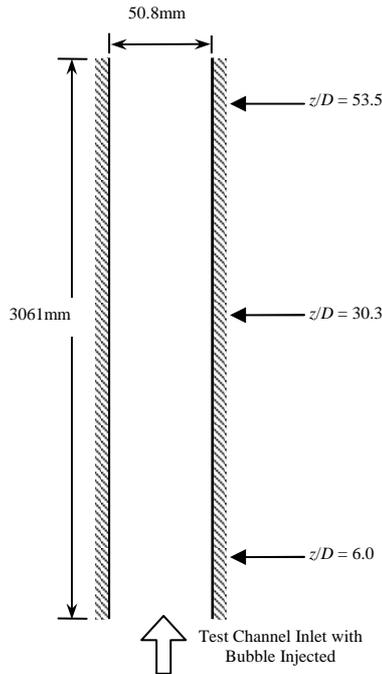Using the above expression, the transport equations become:

$$\frac{\partial(\rho_g \alpha_g f_k)}{\partial t} + \nabla \cdot (\rho_g \alpha_g \bar{u}_g f_k) = b_k \qquad (7)$$

$$\frac{\partial(\rho_g \alpha_g \psi_k)}{\partial t} + \nabla \cdot (\rho_g \alpha_g \bar{u}_g \psi_k) = a_k \qquad (8)$$

The moment transform of the coalescence and break-up of the term S_k can then be expressed as:

$$S_k = B_k^C - D_k^C + B_k^B - D_k^B \qquad (9)$$

where the terms B and D represent the birth and death rates of the coalescence and break-up of bubbles which is equivalent to $S(\xi, t)$ in equation (4). On the basis of the approximation given in equation (6), the birth and death rates can be written as:

$$B_k^C = \frac{1}{2} \sum_i \sum_j N_i N_j (M_i + M_j)^k a(M_i, M_j)$$
$$\qquad (10)$$

$$D_k^C = \sum_i \sum_j M_i^k a(M_i, M_j) N_i N_j \qquad (11)$$

$$B_k^B = \sum_i \sum_j M_i^k b(M_j, M_i) N_j \qquad (12)$$

$$D_k^B = \sum_i \sum_j M_i^k b(M_i, M_j) N_i \qquad (13)$$

Based on equation (10-13), through a series of matrix operations, the source terms a_i and b_i can then be determined and the weights N_i and M_i can be also evaluated according to its definition in terms of f_i and ψ_i. As a preliminary generic study, the birth and death rates are evaluated according to the widely-adopted coalescence kernel by Prince and Blanch (1990) and the break-up mechanism of Luo and Svendsen (1996).

EXPERIMENTAL DETAILS

The two-phase flow experiment conducted by Hibiki et al. (2001) has been performed at the Thermal-Hydraulics and Reactor Safety Laboratory in Purdue University. The test section was a round tube made of acrylic with an inner diameter (D) of 50.8 mm and a length (L) of 3061 mm. The temperature of the apparatus was kept at a constant temperature (20°C) within the deviation of ±0.2°C by a heat exchanger installed in a water reservoir. Local flow

Figure 1: Schematic diagram of experimental arrangement
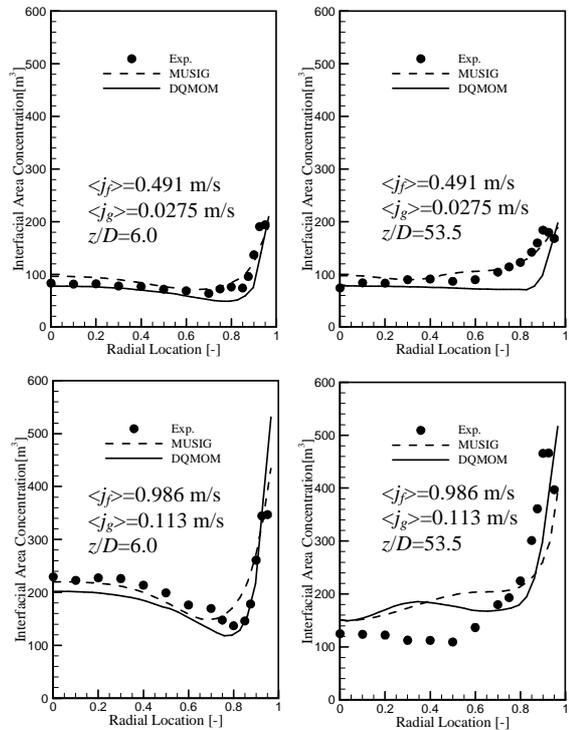
Figure 3: Local predicted and measured interfacial area concentration profiles at $z/D = 6.0$ and 53.5 for both flow conditions
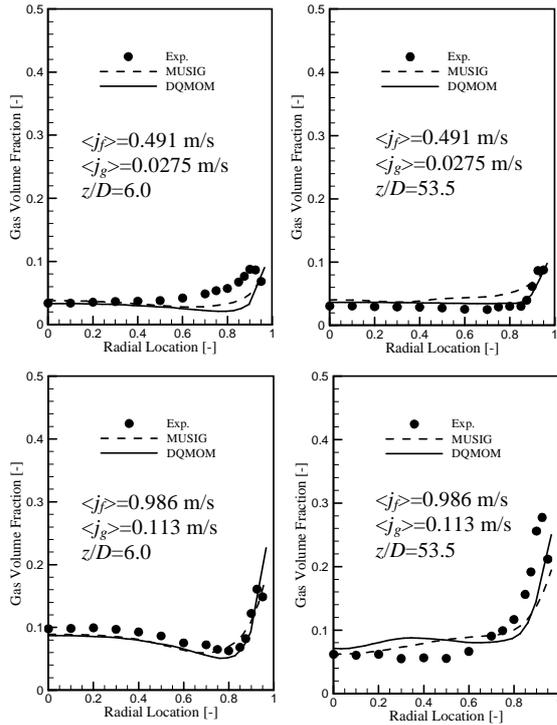
Figure 2: Local predicted and measured void fraction profiles at $z/D = 6.0$ and 53.5 for both flow conditions

measurements using the double sensor and hotfilm anemometer probes were performed at three axial (height) locations of $z/D = 6.0$, 30.3 and 53.5 and 15 radial locations of $r/R = 0$ to 0.95. The schematic diagram of the experimental arrangement is shown in Figure 1. A range of superficial liquid velocities j_l and superficial gas velocities j_g have been performed, which covered mostly the bubbly flow region, including finely dispersed bubbly flow and bubbly-to-slug transition flow regions. Area averaged superficial gas velocity $<j_g>$ was obtained from local void fraction and gas velocity measured by the double sensor probe, whereas area averaged superficial liquid velocity $<j_l>$ was obtained from local void fraction measured by the double sensor probe and local liquid velocity measured by the hotfilm anemometry. More details regarding the experimental set-up can be found in Hibiki et al. (2001). In this paper, numerical predictions have been compared against local measurements at two flow conditions: Case 1 with $<j_l>$=0.491 m/s and $<j_g>$=0.0556 m/s; Case 2 $<j_l>$=0.986 m/s and $<j_g>$=0.113 m/s. The inlet void fractions are 5% and 10% respectively. The bubble size from the air injection is 2.5 mm for both cases.

NUMERICAL DETAILS

For the two-fluid model, two sets of equations governing the conservation of mass and momentum were solved via the ANSYS Inc, CFX-11 computer code. For DQMOM, two sets of transport equations governing four weights and four abscissas were chosen to predict the bubble size distribution of which the evaluation of the source terms a_i and b_i in equations (7) and (8) were determined through matrix operations carried out by an in-house external subroutine. Both breakage and coalescence calibration factors, F_B and F_C, were adjusted to 0.15 and 0.05 respectively. Comparing with our previous study (Cheung

et al., 2007b), F_B and F_C were specified to 1.0 and 0.05 in the MUSIG model based on experimental calibrations. Such discrepancy of calibration factor between both approaches could be attributed to the additional flexibility of the DQMOM. As both weights and abscissas are variables within the DQMOM, calculation of bubble size distribution could be very sensitivity to strength of coalescence and breakage sources. As a result, a different set of calibration factor are adopted in this study. Radial symmetry was assumed, so that the numerical simulations were performed on a 60° radial sector of the pipe with symmetry boundary conditions at both sides. Inlet conditions were assumed to be homogeneous in regards to the superficial liquid and gas velocities, void fractions for both phases and uniformly distributed bubble size in accordance with the flow conditions described above. At the pipe outlet, a relative average static pressure of zero was specified. A three-dimensional mesh containing hexahedral elements was generated resulting in a total of 12,000 elements (i.e. 20 radial, 20 circumferential and 40 axial) covering the entire pipe domain. Reliable convergence was achieved within 600 iterations for a satisfied convergence criterion based on the RMS (Root Mean Square) residuals of 1.0×10^{-4} and for a physical time scale of the fully implicit solution of 0.008 s.

RESULTS AND DISCUSSION

Local radial profiles of the void fraction, interfacial area, Sauter mean diameter, gas and liquid velocities at two measuring axial locations of $z/D = 6.0$ and 53.5 were predicted through the two-fluid model and DQMOM. The computed results are compared against the measured data of Hibiki et al. (2001). In order to assess its predictive capability, additional comparison is also carried out against the predicted MUSIG results obtained through our
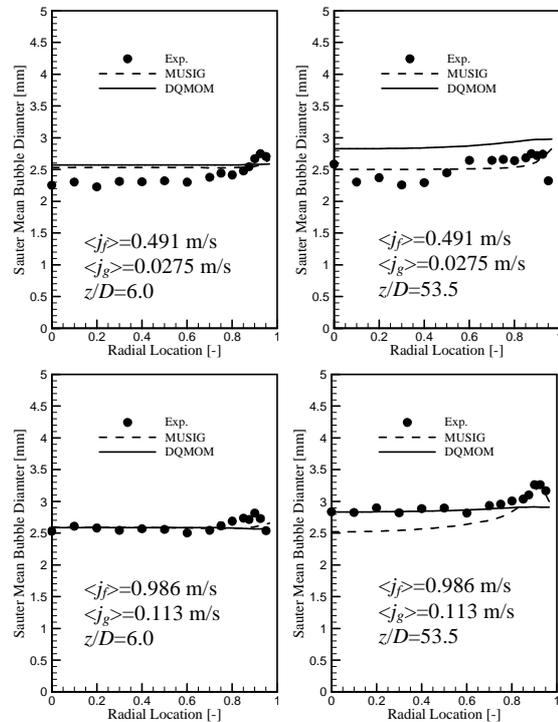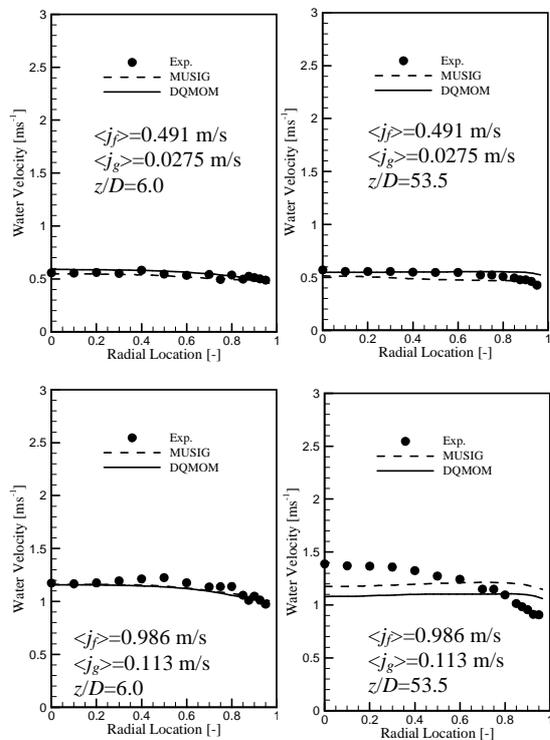

Figure 4: Local predicted and measured sauter mean bubble diameter distributions at $z/D = 6.0$ and 53.5 for both flow conditions
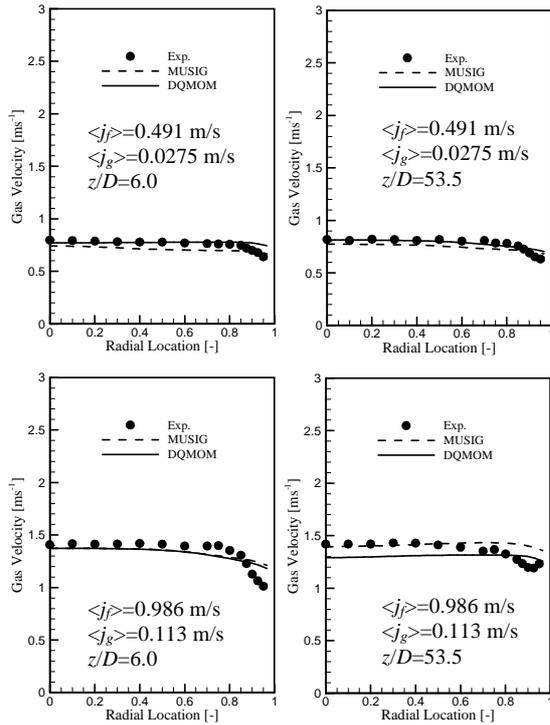
Figure 5: Local predicted and measured gas velocity profiles at *z/D* = 6.0 and 53.5 for both flow conditions

previous work in Cheung et al. (2007b).

Figure 2 shows the void fraction distributions of both flow conditions at the two axial locations for the measured data and computer results of the DQMOM and MUSIG. In isothermal gas-liquid bubbly flows, Serizawa and Kataoka (1990) classified the phase distribution patterns into four

Figure 6: Local predicted and measured liquid velocity profiles at *z/D* = 6.0 and 53.5 for both flow conditions
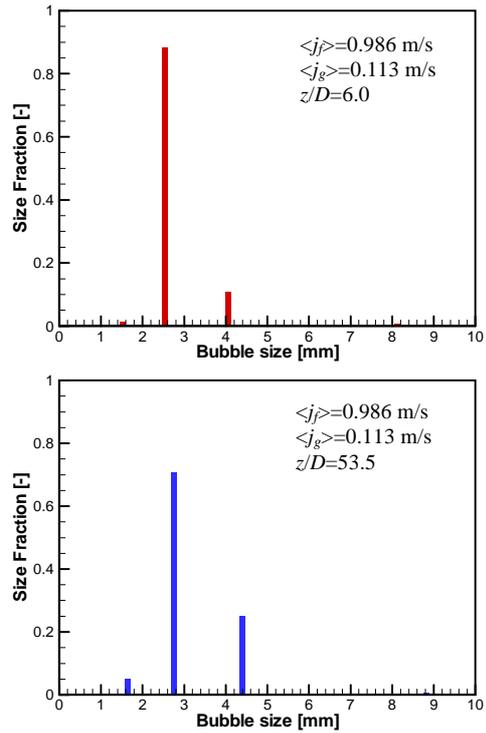
Figure 7: Cross-section averaged bubble size distribution at the axial locations of *z/D* = 6 and *z/D* = 53.5

basic types of distributions: wall peak, intermediate peak, core peak and transition. The void fraction peaking near the pipe wall represented the flow phase distributions caused by the typical wall peak behaviour. In both flow condition, it was observed that the wall peaking profile started to develop at the axial locations of z/D = 6.0 (near the inlet) and become well established at z/D = 53.5 (near the exit). Model predictions of both MUSIG and DQMOM captured the radial void fraction distributions considerably well at the two locations. Nevertheless, it appeared that DQMOM gave slightly better predictions especially at the well-developed wall peaking characteristic at z/D = 53.5 in both test cases.

Figure 3 illustrates the Interfacial Area Concentration (IAC) distributions of both flow conditions at the respective two axial locations for the measurements and the two model predictions. The measured data followed the similar profile as the void fraction distribution as stipulated in Figure 2. Here again, predictions from both MUSIG and DQMOM models were in well agreement with measurements. This further ascertains the predictability of the DQMOM in comparison with MUSIG model. The Sauter mean bubble diameter distributions are exemplified in Figure 4. At *z/D* = 53, good agreement was achieved for DQMOM near the pipe center while MUSIG under-predicted the bubble sizes there. For the flow condition of <*j_l*>=0.491 m/s and <*j_g*>=0.0556 m/s, DQMOM marginally over-predicted the bubble sizes but followed similar trend with the experimental distribution.

Figure 5 and 6 show the local radial gas and liquid velocity distribution at the two axial locations. The introduction of bubbles into the liquid flow had the tendency to flatten the liquid velocity profiles with a relatively steep decrease close to the pipe wall. The same behaviour was also observed for the gas velocity profiles. Overall, both model predictions of the gas and liquid

velocities were in satisfactory agreement with measurements.

The cross-section averaged bubble size distributions near the pipe inlet and near the pipe outlet of the test case $<j_l>$=0.986 m/s and $<j_g>$=0.113 m/s are shown in Figure 7. This figure provided some insight on how the abscissas and weights being evolved in the DQMOM. As can be seen in the two figures, the dominant bubble size was around 2.5mm near the pipe inlet. Through evolution of abscissas and weights in DQMOM, the domain bubble size increased to 2.75mm and the weights of larger bubbles were also increased.

CONCLUSION

A two-fluid model coupled with a population balance model is presented in this paper to handle isothermal gas-liquid bubbly flows. The DQMOM was implemented in the CFD code ANSYS Inc., CFX-11 to determine the temporal and spatial geometrical changes of the gas bubbles. Computed results by the DQMOM two-fluid model were assessed against experiments performed at Purdue University as well as the computed results from the MUSIG two-fluid model. Reasonably good agreements for the void fraction, interfacial area concentration, bubble Sauter mean diameter and gas and liquid velocities have been achieved.

REFERENCES

CHEN, P., SANYAL, J. and DUDUKOVIC, M. P., (2004), "CFD modeling of bubble columns flows: implementation of population balance", *Chemical Eng. Sci.,* **59,** 5201-5207.

CHEUNG, S. C. P., YEOH, G. H. and TU, J. Y., (2007a), "On the modelling of population balance in isothermal vertical bubbly flows - Average bubble number density approach", *Chemical Eng. and Proc.,* **46,** 742-756.

CHEUNG, S. C. P., YEOH, G. H. and TU, J. Y., (2007b), "On the numerical study of isothermal vertical bubbly flow using two population balance approaches", *Chemical Eng. Sci.,* **62,** 4659-4674.

CHEUNG, S. C. P., Yeoh, G. H. and TU, J. Y., (2008), "Population balance modeling of bubbly flows considering the hydrodynamics and thermomechanical processes", *AIChE J.,* **54,** 1689-1710.

HIBIKI, T. and ISHII, M., (2000), "One-group interfacial area transport of bubbly flows in vertical round tubes", *Int. J. of Heat and Mass Transfer,* **43,** 2711-2726.

HIBIKI, T., ISHII, M. AND XIAO, Z., (2001), "Axial interfacial area transport of vertical bubbly flows", *Int. J. of Heat and Mass Transfer,* **44,** 1869-1888.

LO, S. M., (1996). "Application of Population Balance to CFD Modelling of Bubbly Flow via the MUSIG model," AEA Technology, *AEAT-1096*.

LUO, H. and SVENDSEN, H. F., (1996), "Theoretical model for drop and bubble breakup in turbulent dispersions", *AIChE J.,* **42,** 1225-1233.

MARCHISIO, D. L. and FOX, R. O., (2005), "Solution of population balance equations using the direct quadrature method of moments", *J. of Aerosol* Sci.*,* **36,** 43-73.

McGRAW, R., (1997), "Description of aerosol dynamics by the quadrature method of moments", *Aerosol Sci. and Tech.,* **27,** 255-265.

MENTER, F.R., (1994), "Two-equation eddy viscosity turbulence models for engineering applications", *AIAA J.,* **32,** 1598-1605.

PRINCE, M. J. and Blanch, H. W., (1990), "Bubble Coalescence and Break-up in Air-Sparged Bubble-Columns", *AIChE J.,* **36,** 1485-1499.

SATO, Y., SADATOMI, M., SEKOGUCHI, K., (1981), "Momentum and heat transfer in two-phase bubbly flow – I", *Int. J. of Multiphase Flow*, **7,** 167-178.

SERIZAWA, A. and KATAOKA, I., (1990), "Turbulence Suppression in Bubbly 2-Phase Flow", *Nuclear Eng. and Design,* **122,** 1-16.

SUN, X. D., KIM, S., ISHII, M. and BEUS, S. G., (2004), "Modeling of bubble coalescence and disintegration in confined upward two-phase flow", *Nuclear Eng.and Design,* **230,** 3-26.

WANG, T. F., WANG, J. F. and JIN, Y., (2005), "Theoretical prediction of flow regime transition in bubble columns by the population balance model", *Chemical Eng. Sci.,* **60,** 6199-6209.

WU, Q., KIM, S., ISHII, M. and BEUS, S. G., (1998), "One-group interfacial area transport in vertical bubbly flow", *Int. J. of Heat and Mass Transfer,* **41,** 1103-1112.

YAO, W. and MOREL, C,. (2004), "Volumetric interfacial area prediction in upward bubbly two-phase flow", *Int. J. of Heat and Mass Transfer,* **47,** 307-328.